

Study Regarding the Optimal Shape of the Attack Cone for Taps without Channels

Badea LEPĂDĂTESCU✉

Transilvania University of Braşov, Romania, lepadatescu@unitbv.ro

Mihaela MILEŞAN

Transilvania University of Braşov, Romania, mihaela.milesan@unitbv.ro

Abstract

The essence of internal thread forming is the process in which the plastic deformation of the workpiece occurs under the action of the extrusion tap and finally forms the thread. Tap geometry is the most important parameter for a reliable process. Thread forming taps displace material rather than cut or remove it. The taps do not have flutes or cutting edges and therefore no chips are produced. They work with forming edges and spinning dies with polygonal profiles. Since thread forming leads to compression and deformation of the grain, this results in work hardening. The result is increased material strength of the formed thread. The standard tap characteristics are chamfer length, the number of pitches in the chamfer, tap diameter and the number of lobes around a tap section. Each rounded corner of a tap section is referred to as a lobe, where deformation or friction occurs against the inner surface of the previous hole. Hence, the tap section is defined by a curved side polygon that may typically have three, five, or six corners, which are referred to as lobes. The first part of the edge in the direction of rotation that engages the material is the rake edge, which is the part of the edge that suffers abrasion wear. Following the flank actions of the rake, the relief flank that is in contact with the material undergoes abrasion and adhesion wear, as its edge removes material. The paper studies six processing schemes with different attack cones characteristic of the tap without channels, finally concluding on the recommended processing method in different manufacturing cases.

Keywords

taps without channels, attack cone, thread pitch, tapping, plastic deformation, chipping

1. Introduction

Statistical data and specialized literature indicate that 50–70% of taps with sizes up to M18 are rendered inoperative due to the breaking or chipping of the cutting edges on the lead-in (attack) cone.

Tapping by means of plastic deformation eliminates the underlying causes of these failure modes. However, to achieve this, the geometry of the lead-in cone must be carefully designed to ensure smooth tool engagement during the cutting process [1].

Roll taps are stronger than cutting taps due to their design. The effect of a fluteless design produces a large core diameter cross section on the tap. There is no problem with chip jamming like with a cutting tap. This makes roll taps very good against tap breakage.

A Flowdrilled hole may be tapped with conventional cutting taps or, preferably, with cold form Flowtaps. Flowtapping resembles Flowdrill except that the operating temperatures are much lower. Instead of cutting, Flowtaps cold-form the thread no swarf. The process instead of cutting the material displaces the material as the tap runs through the tap area resulting in a smoother and stronger thread.

Tap geometry, Figure 1, is the most important parameter for a reliable process. The standard tap characteristics are chamfer length, the number of pitches in the chamfer, tap diameter and the number of lobes around a tap section.

Three type of lobes are distinguished in each tap:

- i) incremental forming lobes situated in the chamfer area;
- ii) calibration forming lobes around the nominal diameter;
- iii) guiding lobes leading up to the tap shank.

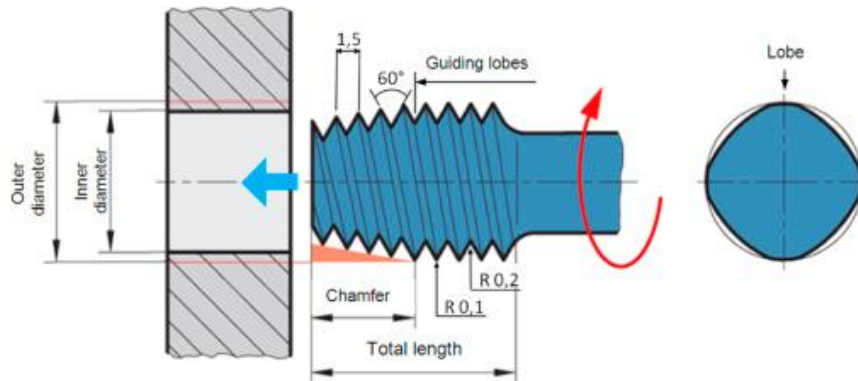


Fig. 1. Terminology and geometry of roll taps

2. Forming Mechanism of Extruded Thread

The essence of internal thread forming is the process in which the plastic deformation of the workpiece occurs under the action of the extrusion tap and finally forms the thread. Figure 2a is a schematic diagram of the workpiece machined by an extruded tap [2].

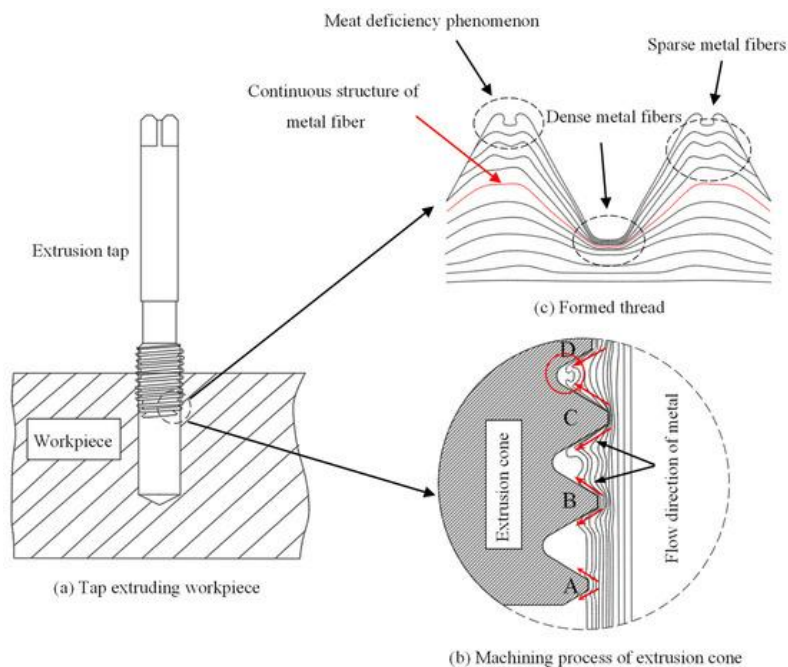


Fig. 2. Schematic diagram of thread machining process.

When the extrusion tap is spun into the workpiece at a certain speed, the inner wall of the workpiece is in contact with the first tooth, A, of the extrusion cone. Because the hardness of the tap is much higher than that of the workpiece, tooth A will extrude a shallow dent on the workpiece surface. The metal of the workpiece is plastically deformed by the extrusion of tooth A, which flows along both sides of tooth A and forms a bulge on both sides of the top of it. As the tap rotates once during the working process, the tap moves forward by a distance of pitch, and tooth B enters the indentation extruded by tooth A. Because there is a certain cone angle in the extrusion cone of the tap, the depth of tooth B is deeper than that of tooth A. With tooth C being squeezed into the workpiece, the dent left by tooth B is further extruded, and the amount of metal material flowing into the groove between teeth B and further increases. At this time, there will be a preliminary outline of the thread between teeth B and C. As the last tooth, D, of the extrusion cone is extruded into the workpiece, the degree of plastic deformation of the workpiece further increases, and the amount of metal material extruded between the two teeth further increases. At this point, a thread with high integrity and that is close to the qualified size will be

formed between teeth C and D. The forming process of the thread under the action of the tap extrusion taper is shown in Figure 2b [3].

3. Possible Shapes of The Lead-In Cone

Initially, six machining schemes with different lead-in cone shapes – characteristic of taps without flutes – are proposed, Figure 3 [1].



Fig. 3. Machining schemes with different attack cone geometries, specific to taps without flutes

A detailed analysis of these schemes reveals the following observations:

For *a* shape, the deformation occurs in inclined layers, oriented at a certain angle to the symmetry axis of the semi-finished product. In this case, the attack cone is formed on the outer diameter (Figure 4).

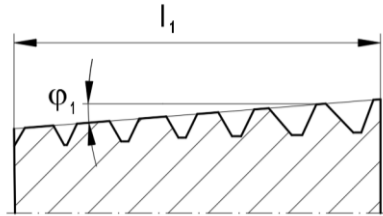


Fig. 4. Attack cone formed on the outer diameter

This processing scheme is also significantly influenced by the thread pitch, even when the cone is formed on the pitch diameter. As shown in Figure 5, the attack cone exhibits a thread pitch excess *x*, which results in the described processing scheme [4].

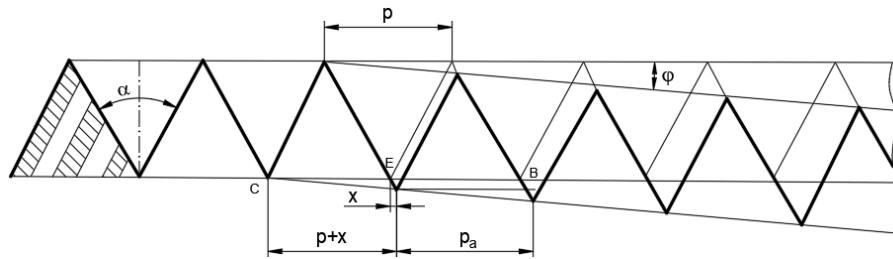


Fig. 5. Processing scheme influenced by thread pitch (attack cone on the pitch diameter)

This excess is calculated as follows:

$$\operatorname{tg} \varphi = \frac{AB}{p_a} \quad (1)$$

resulting:

$$p_a = \frac{AB}{\operatorname{tg} \varphi} = \frac{p_a \cdot DE}{\frac{p}{2} + x} \cdot \frac{1}{\operatorname{tg} \varphi} \quad (2)$$

but:

$$\frac{DE}{y} = \frac{\frac{p}{2} + x}{p_a} \quad (3)$$

Relationship (3) is derived from the similarity of triangles $\triangle CDE$ and $\triangle ABD$.

This leads to the final result:

$$X = \frac{\frac{p}{2}}{\operatorname{ctg} \varphi \cdot \operatorname{ctg} \frac{\alpha}{2} - 1} \quad (4)$$

In this case:

$$p_a = p_{\max} \quad (5)$$

The attack cone shape *b* exhibits the same characteristics; however, in this case, as shown in Figure 6, we have:

$$p_a = p_{\min} \quad (6)$$

and

$$X = \frac{\frac{p}{2}}{\operatorname{ctg} \varphi \cdot \operatorname{ctg} \frac{\alpha}{2} + 1} \quad (7)$$

If the attack cone is executed according to options (a) or (b), an asymmetric deformation of the material is obtained, which leads to an uneven load transfer from the inner thread course [3].

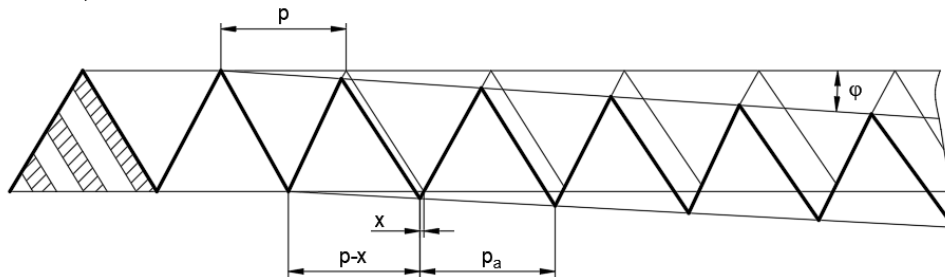


Fig. 6. Processing scheme illustrating the influence of thread pitch (attack cone positioned on the mean diameter)

If the attack cone is executed according to options (a) or (b), an asymmetric deformation of the material is obtained, which leads to an uneven load transfer from the inner thread course [5].

For *c* shape of the attack cone, the processing scheme is obtained by a combination of two attack cones: $\varphi_1 = 3^\circ$ executed on the middle diameter and $\varphi_2 = 10^\circ$ executed on the outer diameter (Figure 7).

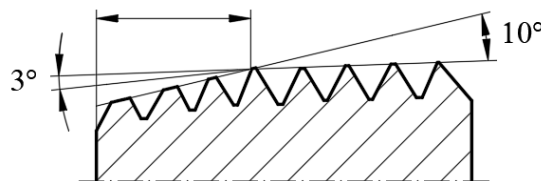


Fig. 7. Combination of two attack cones made on the same length

The deformation scheme shows the asymmetry of the layers. This fact leads to the non-uniformity of the loads taken on the working turns of the inner thread.

The *d* shape of the attack cone is a combination of two attack cones with angles $\varphi_1 = 3^\circ$ executed on the middle diameter, and $\varphi_1 = 1^\circ 50'$ on the outer diameter. The first part works according to scheme *a*, and the other two, according to scheme *e* (Figure 8).

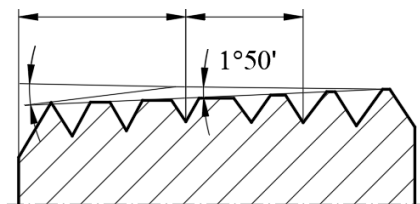


Fig. 8. Combination of two attack cones made on different lengths

The scheme has the disadvantage that the forces increase as the semi-finished product is processed. For *e* shape, the attack cone is made on the average diameter (Figure 9).

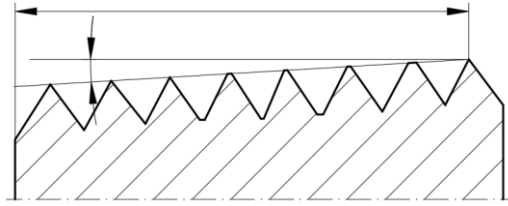


Fig. 9. Attack cone made on the medium diameter

According to Figure 10:

$$p_a = p \quad (8)$$

$$x = \frac{p}{2} \operatorname{tg} \varphi \cdot \operatorname{tg} \frac{\alpha}{2} \quad (9)$$

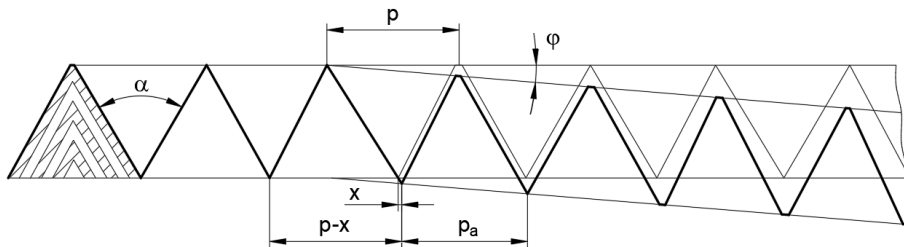


Fig. 10. Processing scheme due to thread pitch concordance

The metal deformation is done in symmetrical steps with respect to the symmetry axis of the semi-finished product. The correlation of the parameters must be taken into account: the pitch *p*, the angle φ and the length of the attack cone.

The limitation of the attack cone length is given by the processing of the blind holes. For this, the form *f* is used [4].

Considering that the chipping moment is reduced by increasing the angle φ of the attack cone, it is advantageous to work with a shorter length.

But at a length that is too short (Figure 11), the tap experiences a large axial resistance oriented in the opposite direction of the movement, which causes an unsafe guidance (Figure 12).

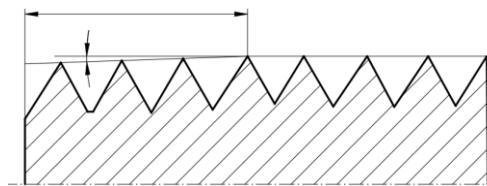


Fig. 11. Attack cone made on the average diameter at a shorter length

The higher the hardness of the material being threaded, the higher will be the forces F_a and F . Therefore, for soft material it is recommended $\varphi = 8 - 10^\circ$ ($\sigma_r < 270 \frac{\text{kgf}}{\text{mm}^2}$) while for hard material, $\varphi = 6 - 8^\circ$ ($\sigma_r < 70 \frac{\text{kgf}}{\text{mm}^2}$).

Correlating with the cross-section parameters, the optimal value $\varphi = 8^\circ$ is considered. Shapes *e* and *f* of the attack cone take the stresses equally on both flanks of the thread, giving it a minimum torsional moment.

A secondary phenomenon consists of material deposits on the working turns of the thread.

For difficult working conditions, it is recommended that before the rectification operation, a channel of small width and depth is made, which facilitates the penetration of the cooling-lubricating liquid.

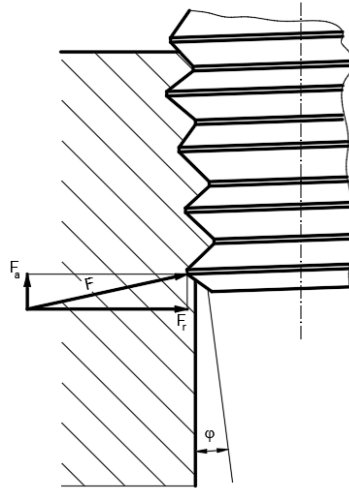


Fig. 12. Scheme of forces acting in the deformation process

Taps without pitch error represent the ideal case. In reality, the pitch of the thread in the deformation schemes *e* and *f* will not be offset in the lower part of the cone $X = 0$, but in the upper part (Figure 13).

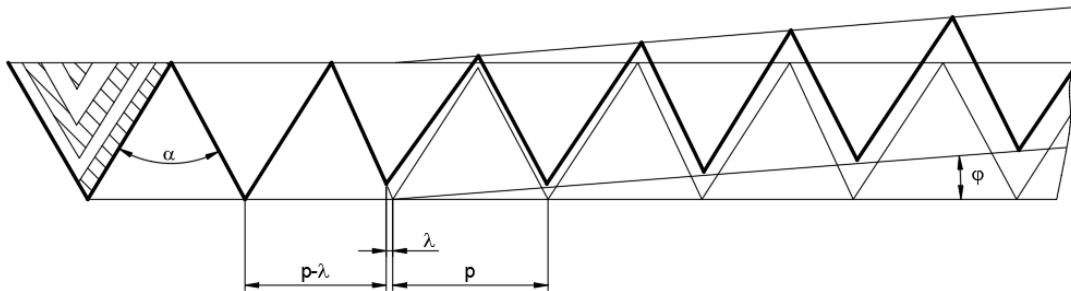


Fig. 13. Real machining scheme with linear attack cone executed on the pitch diameter

Step error will be:

$$y = \frac{p}{2} \cdot \operatorname{tg} \varphi \cdot \operatorname{tg} \frac{\alpha}{2} \quad (10)$$

and

$$p_a = p \left(1 - \frac{\operatorname{tg} \varphi \cdot \operatorname{tg} \frac{\alpha}{2}}{2} \right) \quad (11)$$

For a better uniformity of taking over the loads on the working thread course, an attack cone in the shape of a circular arc can also be executed (Figure 14).

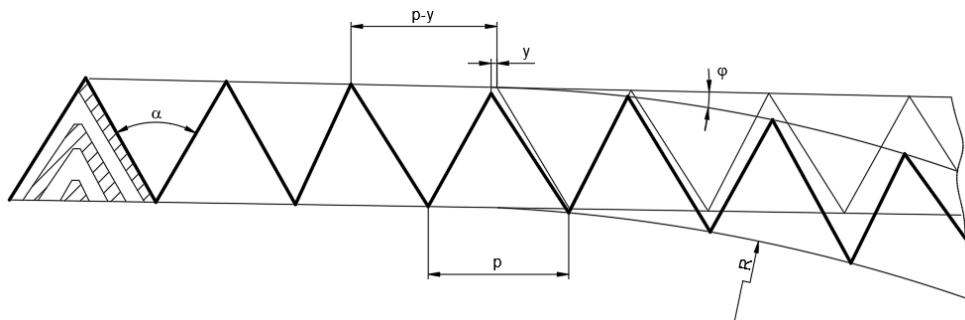


Fig. 14. Actual machining scheme with a cone located on the pitch diameter, shaped as a circular arc ($X = 0$)

According to Figure 14:

$$y = \frac{R - \sqrt{R^2 - p^2}}{2} \cdot \operatorname{tg} \frac{\alpha}{2} \quad (12)$$

$$p_a = p - \frac{R - \sqrt{R^2 - p^2}}{2} \cdot \operatorname{tg} \frac{\alpha}{2} \quad (13)$$

The attack cone shown in Figure 14 obtains minimum moment and axial stresses.

3. Conclusions

As a result of the analysis, the following conclusions can be drawn:

1. Attack cones executed on the outer diameter (shapes a and b) are simple from a design perspective but cause asymmetric material deformation;
2. Forms c and d of the attack cone are relatively difficult to manufacture and introduce internal stresses within the threaded joint;
3. Shapes e and f represent the ideal case, ensuring symmetrical and uniform deformation, minimal torque, and consequently, the formation of precise threads. Considering the advantages of attack cone types e and f, the solution most commonly applied for through holes is the linear attack cone located on the pitch diameter, with minimal pitch deviations (see Figure 13). For blind holes, the use of a circular-arc-shaped cone on the pitch diameter is recommended.

References

1. Elósegui I., López de Lacalle L.N. (2010): *Threading on ADI cast iron, developing tools and conditions*. AIP Conference Proceedings, eISSN 1551-7616, Vol. 1315, is. 1, pp. 116-121, <https://doi.org/10.1063/1.3552340>
2. de Carvalho A.O., Brandão L.C., Panzera T.H., Lauro C.H. (2012): *Analysis of form threads using fluteless taps in cast magnesium alloy (AM60)*. Journal of Materials Processing Technology, eISSN 1873-4774, Vol. 212, is. 8, pp. 1753-1760, <https://doi.org/10.1016/j.jmatprotec.2012.03.018>
3. Ivanov V., Kirov V. (1997): *Rolling of internal threads: Part 1*. Journal of Materials Processing Technology, eISSN 1873-4774, Vol. 72, is. 2, pp. 214-220, [https://doi.org/10.1016/S0924-0136\(97\)00171-4](https://doi.org/10.1016/S0924-0136(97)00171-4)
4. Blazynski T.Z. (1989): *Plasticity and Modern Metal-forming Technology*. Springer Dordrecht, ISBN 978-1-85166-272-2
5. Agapiou J.S. (1994): *Evaluation of the effect of high speed machining on tapping*. Journal of Manufacturing Science and Engineering, eISSN 1528-8935, Vol. 116, pp. 457-462, <https://doi.org/10.1115/1.2902128>

Paper presented at the 17th International Conference
 “STANDARDIZATION, PROTOTYPES and QUALITY: A means of Balkan Countries’ collaboration”